Band alignment in $LaAlO_3/SrTiO_3$ oxide heterostructures inferred from hard x-ray photoelectron spectroscopy

G. Berner,[1] A. Müller,[1] F. Pfaff,[1] J. Walde,[1] C. Richter,[2,3] J. Mannhart,[3] S. Thiess,[4] A. Gloskovskii,[4] W. Drube,[4] M. Sing,[1] and R. Claessen[1,*]

[1]*Physikalisches Institut and Röntgen Center for Complex Materials Systems (RCCM), Universität Würzburg, Am Hubland, D-97074 Würzburg, Germany*

[2]*Institute of Physics, Universität Augsburg, Electronic Correlations and Magnetism, Experimentalphysik VI, Universitätsstraße 1, D-86135 Augsburg, Germany*

[3]*Max Planck Institute for Solid State Research, Heisenbergstraße 1, D-70569 Stuttgart, Germany*

[4]*DESY Photon Science, Deutsches Elektronen-Synchrotron, D-22603 Hamburg, Germany*

(Received 3 July 2013; published 6 September 2013)

We present a detailed study of the electronic structure and band alignment in $LaAlO_3/SrTiO_3$ oxide heterostructures by hard x-ray photoelectron spectroscopy. Our spectroscopic measurements find no evidence for the strong potential gradient within the polar $LaAlO_3$ film predicted by band theory. Due to the high interface sensitivity of the method, we are further able to determine the valence band offset between the $LaAlO_3$ film and the $SrTiO_3$ substrate, which is found to be independent of the number of LAO overlayers. Finally, we discuss several explanations for the apparent absence of the built-in field in *ex situ* prepared $LaAlO_3/SrTiO_3$ heterostructures.

DOI: 10.1103/PhysRevB.88.115111 PACS number(s): 73.20.−r, 79.60.Jv, 73.50.Pz

I. INTRODUCTION

By breaking the translation or inversion symmetry at the interface, oxide heterostructures may reveal unexpected and novel functionalities. A prominent example is the formation of a high-mobility two-dimensional electron system (2DES) at the interface of the polar $LaAlO_3$ (LAO) grown epitaxially on TiO_2-terminated nonpolar $SrTiO_3$ (STO), when the LAO overlayer thickness exceeds three unit cells (uc).[1,2] The 2DES is switchable by an external electric field[2] and undergoes a transition to a two-dimensional superconducting ground state below 0.2 K.[3,4] Recently, the coexistence of a superconducting state and ferromagnetism was experimentally observed.[5–7] While oxygen defects[8] or cation intermixing at the interface[9,10] have also been suggested as origin of the 2DES, the most discussed explanation is electronic reconstruction driven by the polar discontinuity between both oxides. In this scenario, electrons are transferred from the surface to the interface to compensate the built-in potential within the polar LAO film.[11] These extra electrons are confined to the interface and hosted in otherwise unoccupied Ti 3*d* states.[11–13]

Recent density functional theory (DFT) calculations of the layer-resolved density of states (LDOS) support this picture.[14,15] It is found that the polar field within the LAO causes the O 2*p*-derived valence band to assume a strong gradient towards the chemical potential. With increasing LAO thickness, the valence band maximum eventually crosses the chemical potential at the LAO surface, depleting these states and transferring electrons to the next available empty states, namely, the STO conduction band states at the interface, thus forming a Ti 3*d*-derived conducting 2DES.

While the DFT results provide a coherent explanation for the 2DES formation, direct experimental evidence for the electronic reconstruction scenario and the related band bending in LAO is still lacking. Hard x-ray photoelectron spectroscopy (HAXPES) with its high probing depth and interface sensitivity is a suitable tool to address this issue. It provides detailed information on the electronic structure of the entire heterostructure, i.e., both in the LAO film *and* the STO substrate. In particular, the method is very sensitive to composition at the interface[13] and is in principle capable of detecting a built-in potential, as has been demonstrated for other polar oxide heterostructures.[16]

In this paper, we study the electronic structure in LAO/STO heterostructures by comprehensive HAXPES experiments. Based on a detailed analysis of valence band and core-level spectra, we address the question of the band bending within the LAO film as well as the band alignment between STO and LAO. The spectroscopic findings are found to deviate from the conventional electronic reconstruction picture suggested by DFT. We discuss possible intrinsic and extrinsic explanations for the observed discrepancies. In particular, we point out that oxygen vacancies on the LAO surface may play a crucial role in a modified electronic reconstruction scenario explaining the 2DES formation consistent with our spectroscopic observations.

II. EXPERIMENT

The HAXPES experiments were performed at the P09 beamline of PETRA III (DESY, Hamburg), using a SPECS Phoibos 225 spectrometer with an overall energy resolution of $\Delta E \approx 0.45$ eV at a photon energy of 3.5 keV. For complementary XPS measurements, a monochromatized Al $K\alpha$ laboratory source ($h\nu = 1486.6$ eV) and an Omicron EA-125 analyzer were used. Here, the overall energy resolution was ≈0.40 eV. Both spectrometers were stable in the required energy range within ±0.02 eV. As energy reference, a Au Fermi edge was measured. If not otherwise indicated, all spectra were taken at room temperature (RT) and in normal emission geometry.

A set of LAO/STO samples with varying LAO overlayer film thickness (2, 4, 5, 6, 12, and 20 uc) was prepared by pulsed laser deposition (PLD) on TiO_2-terminated STO substrates creating an *n*-type interface. A detailed description

of sample growth can be found in Ref. 2. The film thickness was monitored by reflection high-energy electron diffraction (RHEED). The oxygen pressure during growth was set to 1×10^{-4} mbar while the substrate temperature was held at 780 °C. Subsequently, a post-oxidation procedure was applied, where the samples were cooled down to room temperature in 0.4 bar of oxygen. Transport measurements previously done on the samples have shown that the interface becomes conducting only at a critical thickness of $\geqslant$4 uc hosting highly mobile electrons.[2,17] All samples are equipped with a gold contact as used in transport measurements.[2] This provides a good electrical contact between the interface 2DES and the sample holder to overcome charging effects during the photoemission process. As reference samples for bulk STO and LAO spectra we used a bare Nb-doped STO substrate (0.05 wt.%) and a thick LAO film (20 uc), respectively. All samples were transported under ambient atmosphere and measured without any further surface preparation.

III. RESULTS

A. Potential gradient in $LaAlO_3$

The electronic reconstruction picture predicted by the DFT calculations would have several consequences which are in principle detectable by photoemission, as schematically depicted in Fig. 1: (i) Due to the potential gradient in the LAO film valence band states will be pushed all the way to (and above) the chemical potential μ, i.e., spectral weight should be observed at or near the chemical potential due to the occupied states in the LAO surface layer. (ii) All atomic core levels in the LAO film will track the finite slope of the valence band edge, with the corresponding spectra thus being broadened and shifted in energy relative to a flat band situation. As an example, Fig. 1 sketches the expected valence band and core-level spectra for the case of a conducting 6-uc sample. Furthermore, the core-level spectra for varying LAO film thicknesses should show a significant change in the peak shape because the rising number of LAO layers beyond the critical thickness leads to an increasing amount of transferred electrons, thereby reducing the built-in field and hence also the relative core-level energy shift between adjacent LAO layers.

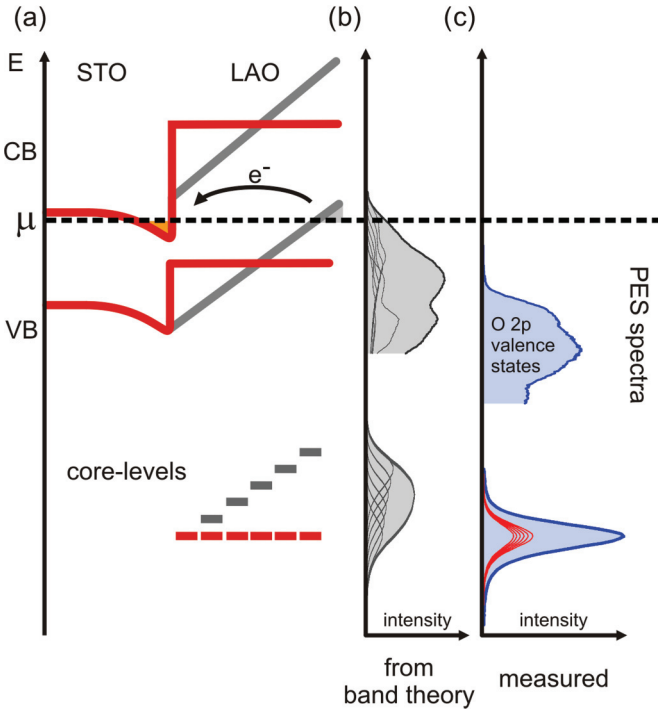

FIG. 1. (Color online) (a) A simplified band diagram demonstrating the behavior of both the valence band and the core levels, as affected by electronic reconstruction. It shows the gradient in the LAO band edges for the ideal case predicted by band theory (gray) and compares it to the flat band situation derived from our photoemission study (red). Sketches of the photoemission spectra reflecting the band situation from DFT (b) and as actually measured (c), including relative energetic shifts and exponential damping of the photoemission spectra of each layer (for details see text).

We start our experimental investigations with an analysis of the LAO/STO valence band spectra. In Fig. 2(a), the valence band spectrum of a conducting 6-uc sample is presented. As is clearly evident, a wide gap between the chemical potential and the valence band edge appears. We determine the energy position of the valence band maximum (VBM) by a linear fit of the valence band edge to be $\approx$3.1 eV. This value is practically independent of the LAO film thickness for all conducting heterostructures studied here, i.e., between 4 and 20 uc (see Table I). For the nonconducting 2-uc sample, no reliable VBM energy could be determined because charging effects prevented a precise measurement within acceptable error bars. The absence of any spectral weight just below the chemical potential and the large photoemission gap of 3.1 eV already indicate the absence of the predicted potential gradient.

To confirm this result, we additionally measured the spectra of several core levels. As an example, we show in Fig. 2(b) the Al 1*s* spectra. We do not observe any significant modification of the peak shape, e.g., broadening or asymmetry, as a function of LAO film thickness. For a more quantitative analysis, we introduce a model to describe how the predicted potential gradient would influence the peak shape of the Al 1*s* spectrum. In this model, the total spectrum is composed out of the contributions of each individual LAO layer, with each layer shifted in energy with respect to the bulk position and multiplied with the damping factor $e^{-z/\lambda}$ to include the depth sensitivity of photoelectron spectroscopy. Here, z describes the depth from which the photoelectrons are emitted and λ the inelastic mean-free path of the photoelectrons. For the Al 1*s* core level and the used photon energy (3.5 keV), λ is approximately 30 Å according to the NIST database.[18] As underlying reference line shape for each single layer, we have used the Al 1*s* bulk spectrum of the LAO reference sample.

The resulting model spectrum for a typical shift of 0.4 eV per uc, as e.g. predicted for a 5-uc sample,[14] is shown in Fig. 2(b) as gray shaded curve. It displays both a clear asymmetry and a peak shift from the expected bulk binding energy, which is absent from the experimental spectra. From this comparison and within the experimental uncertainties we estimate an upper limit for a possible internal field-induced energy shift of at most 6 meV per uc. The strong deviation from the DFT result is consistent with other photoemission studies on LAO/STO heterostructures.[10,19–22]

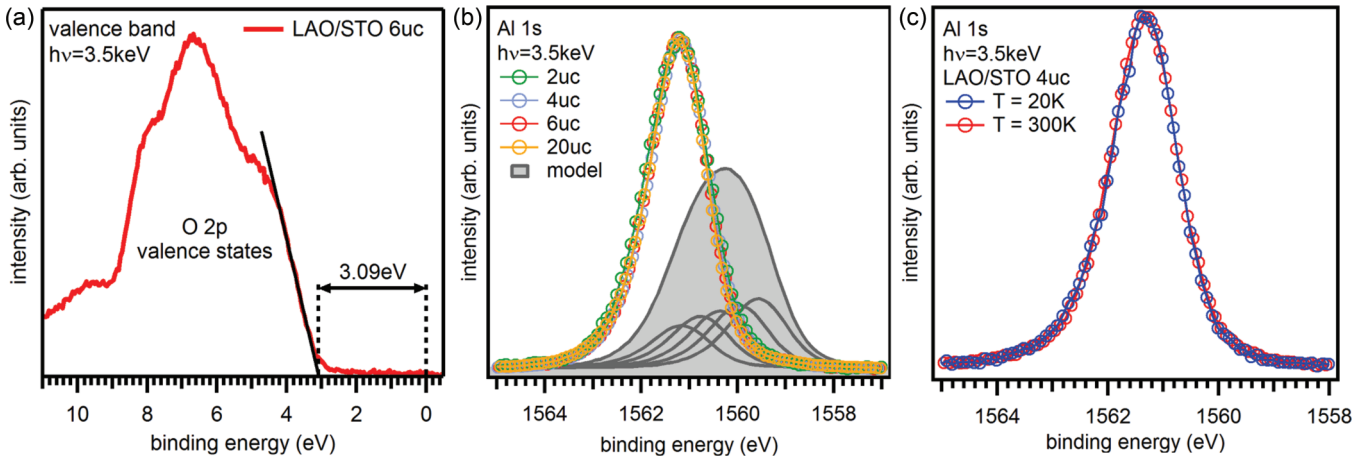

FIG. 2. (Color online) (a) The valence band spectrum shows a large gap between chemical potential and the VBM. The black line indicates the linear extrapolation of the spectral onset used for the determination of the VBM energy. (b) Al 1*s* core-level spectra measured for various thicknesses of the LAO film. No changes in peak shape can be observed. For comparison, also a model spectrum as expected in the presence of an internal field is shown (gray shaded); see text for details. All spectra are normalized to the same integrated peak area. (c) Al 1*s* core-level spectrum of a 4-uc sample as function of temperature. No changes occur between 20 and 300 K.

In order to rule out temperature effects as the origin of this discrepancy, we have measured the Al 1*s* core-level spectrum over a wide temperature range between 20 and 300 K. As shown in Fig. 2(c), no notable changes can be observed.

B. Band bending in $SrTiO_3$

According to DFT band theory, the STO conduction band minimum (CBM) bends below the chemical potential near the interface to form a potential trough with a width of a few unit cells only ($T = 0$ K).[15,23–26] The resulting Ti 3*d*-derived quantum-well states become populated by the electronic reconstruction mechanism and form the 2DES. The Ti 3*d* character of the interfacial carriers has experimentally been verified by several spectroscopic studies.[11,13,27] As an example, Fig. 3(a) shows the Ti 2*p* core-level spectrum of a 4-uc LAO/STO sample which besides a dominant Ti $2p_{3/2}$ peak corresponding to Ti^{4+} (arising mainly from the STO bulk) displays a slight shoulder at lower binding energy (≈457 eV) which can be assigned to the chemically shifted photoemission from Ti^{3+} ions at the interface, thereby giving direct evidence of occupied Ti 3*d* states.[13]

Concerning the magnitude of the actual band bending, the DFT calculations yield a value of more than 0.5 eV within the first five STO layers.[15,25,26] In order to test this prediction experimentally, we have analyzed the substrate core levels. However, with the Ti 2*p* line shape being affected by the Ti^{3+} shoulder and the other Ti and Sr core levels being rather broad and/or of small intensity, the Sr 3*d* doublet is most suitable for our analysis. The corresponding spectrum of a 6-uc sample is shown in Fig. 3(b), compared to one taken from a Nb-doped STO reference sample. For the LAO/STO sample, some background corrections have been made because the Sr 3*d* doublet is affected by a satellite emission of the La 4*d* core level. No significant broadening or asymmetry with respect to the reference sample is observed, indicating that the actual band bending is far less than theoretically predicted. Applying a model similar to the core-level analysis of internal field effects in the Al 1*s* spectra, we derive an upper limit for the STO band bending of approximately ±0.3 eV within the information depth of HAXPES. Note, however, that the core-level energies follow the VBM and that for our analysis we have additionally assumed a constant energy separation between the VBM and the CBM. If, however, the fundamental band gap slightly shrinks towards the interface, the small energy shifts estimated from the core-level energies may still allow for a stronger bending of the STO CBM. Indeed, several DFT calculations seem to indicate such a gap renormalization towards the interface.[23,28]

TABLE I. (Upper part) Values for the energy position of the LAO VBM and the experimental energy differences as required for the determination of the valence band offsets. (Lower part) Valence band offsets derived from the valence band and core-level (CL) analysis, respectively. Because no dependence on the LAO film thickness is observed, mean values from both methods can be quoted.

	Nb-STO	4 uc	5 uc	6 uc	12 uc	20 uc	Mean value
VBM (±0.1 eV)	3.31	3.13	3.10	3.09	3.14	3.07	
ΔE(Al 2*p*–VBM) (±0.1 eV)		71.22	71.21	71.28	71.31	71.33	
ΔE(Sr $3d_{5/2}$–VBM) (±0.1 eV)	130.60	130.83	130.85	130.94	130.86		
ΔE(Sr $3d_{5/2}$–Al 2*p*) (±0.1 eV)		59.61	59.64	59.66	59.55		
ΔE_{VB} from VB analysis (±0.1 eV)		−0.41	−0.33	−0.37	−0.31		−0.36
ΔE_{VB} from CL analysis (±0.1 eV)		−0.34	−0.37	−0.39	−0.28		−0.35

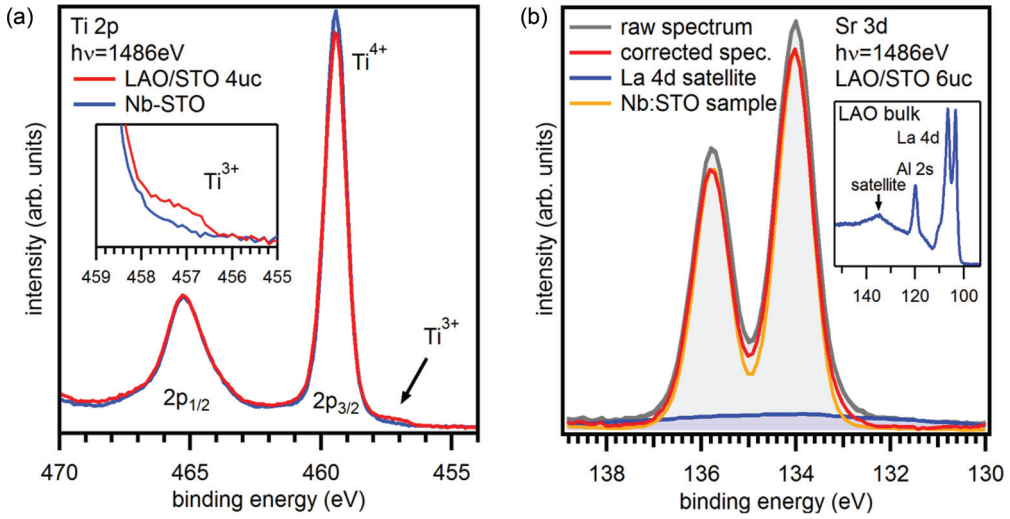

FIG. 3. (Color online) (a) Measured Ti $2p$ core-level spectrum of a 4-uc LAO/STO sample and of a Nb-doped reference sample. The spectra are normalized to the same peak area. A chemically shifted Ti^{3+} emission is observed, which reflects the extra Ti $3d$ electrons hosted at the interface. (b) The Sr $3d$ core-level spectrum exhibits no significant broadening with respect to the Nb-doped STO sample, thus no indication for strong band bending is found. Note that a background correction is needed for an accurate analysis since a La $4d$ satellite emission at ∼134 eV overlaps with the Sr $3d$ doublet (see inset).

C. Band alignment at the interface

The HAXPES sensitivity for both the LAO film *and* the STO substrate allows us to investigate the relative arrangement of the VBM on both sides of the interface, i.e., the valence band offset. Several theoretical studies have addressed the band alignment and predict an offset, where the VBM of STO is *above* that of LAO,[23,24,29] generally denoted as a type-I interface. Other groups come to the contrary results, with the VBM of STO *below* the VBM of LAO (type-II interface).[15]

Experimentally, the relative band offset can be determined by two independent methods. The first one involves a decomposition of the valence band spectrum into the individual LAO and STO contributions. For this purpose, the valence band of the heterostructure is fitted by a superposition of the valence bands measured on the bulk components. The free parameters to be determined in the fitting procedure are (i) the energetic shift between both bulk valence bands and (ii) their relative intensity. Because the valence band of both oxides is dominated by O $2p$ states, it is important to measure them with bulk-sensitive HAXPES ($h\nu = 3.5$ keV) in order to minimize any distorting effects by oxygen-containing surface adsorbates. Note that under these conditions, the (small) band bending in the first STO layers is negligible since most of the spectral weight arising from STO stems from deeper layers in the bulk.

The result for the 5-uc sample is shown in Fig. 4(a). The best agreement between superposed bulk spectra and the measured LAO/STO valence band is obtained for a band offset of -0.33 ± 0.10 eV. The negative sign corresponds to a type-II situation. The obtained offsets for the other samples are presented in Table I. The values show some slight scatter, but no obvious trend with varying LAO film thickness can be discerned within the error bars. Thus, an average band offset of -0.36 ± 0.10 eV is obtained.

The relative valence band intensity I_{STO}/I_{LAO} gathered from these fits is expected to systematically decrease as a function of LAO film thickness. Taking into account the damping factor $e^{-d/\lambda}$ and assuming that $\lambda_{STO} \approx \lambda_{LAO} = \lambda$, the intensity ratio can be described by

$$\frac{I_{STO}}{I_{LAO}} = \frac{1}{\exp\left(\frac{d_{LAO}}{\lambda}\right) - 1}. \quad (1)$$

Figure 4(b) shows the calculated I_{STO}/I_{LAO} as a function of the LAO film thickness using a λ of approximately 50 Å (calculated from NIST database[18]). The I_{STO}/I_{LAO} values of various samples obtained from the valence band fits are also plotted in the chart. The excellent correspondence between theoretical and fitted intensity ratios emphasizes the high reliability of our above valence band analysis.

In an alternative approach, the band offset can also be determined by an analysis of the core-level spectra. For that, the energy difference between a core level and the valence band maximum has to be measured in both bulk components. The same core levels have to be measured in the heterostructures, accordingly. From these data, one can calculate the valence band (VB) offset and, by including the band gaps Δ of LAO and STO, also the conduction band (CB) offsets:[30,31]

$$\Delta E_{VB} = \left(E_{Sr\,3d_{5/2}} - E_{VBM}\right)_{STO} - \left(E_{Al\,2p} - E_{VBM}\right)_{LAO} - \left(E_{Sr\,3d_{5/2}} - E_{Al\,2p}\right)_{LAO/STO}, \quad (2)$$

$$\Delta E_{CB} = \Delta_{LAO} - \Delta_{STO} - \Delta E_{VB}. \quad (3)$$

The Al $2p$ core level was measured on the LAO reference sample, the Sr $3d$ core level on the Nb-doped STO reference sample, as well as both core levels on the heterostructures (see Fig. 4). The evaluated energy differences as well as the calculated values for the VB offset of our set of samples are summarized in Table I. Similar to the results from the valence band analysis, no dependence on LAO film thickness can be found within the error bars. In our measurements, the energy difference between the Sr $3d$ and the Al $2p$ core levels is nearly constant. The resulting mean value of the VB offsets is -0.35 ± 0.10 eV, in excellent agreement with that determined

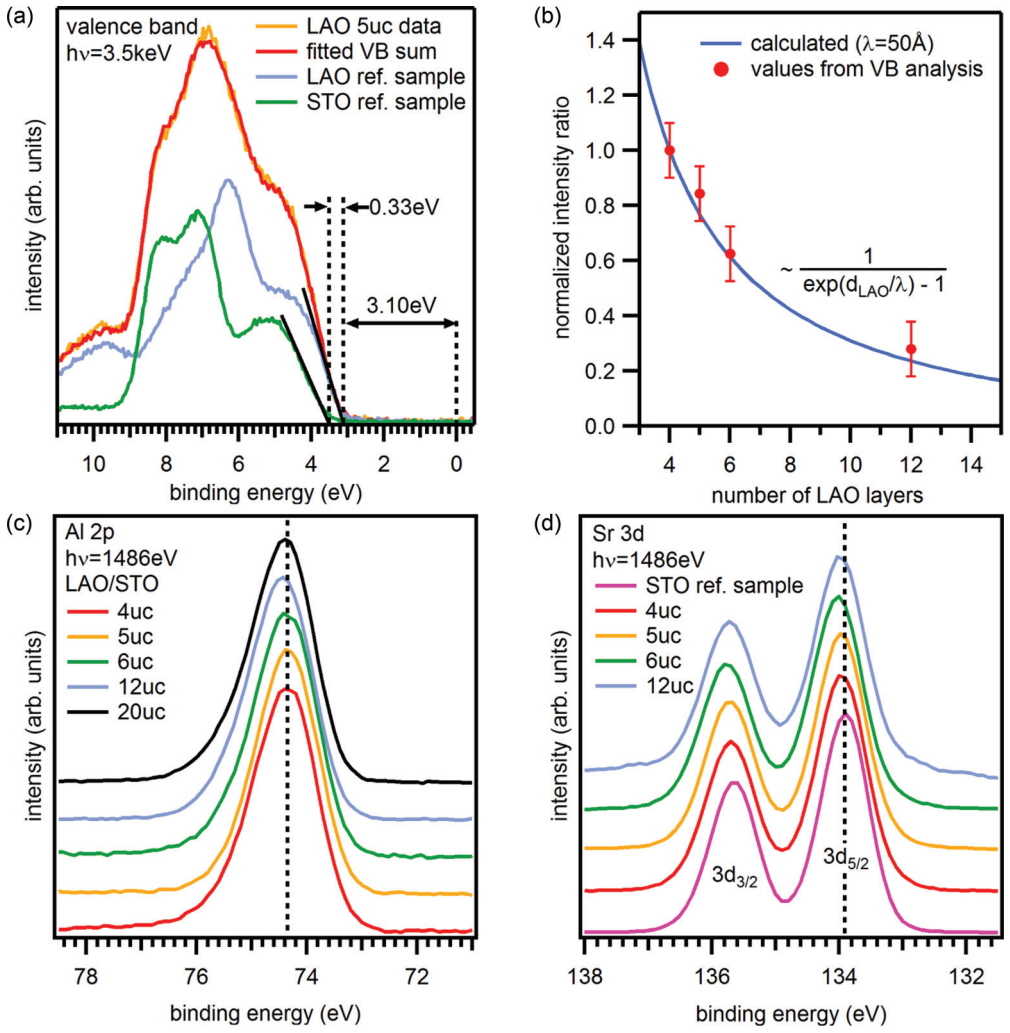

FIG. 4. (Color online) (a) Valence band spectrum of a 5-uc LAO/STO heterostructure and its decomposition into the individual LAO and STO contributions (see text for details). The black lines indicate the determination of the respective VBM energies. (b) Relative valence band intensity ratio I_{STO}/I_{LAO} derived from the valence band analysis of several samples compared to its theoretical value as function of LAO film thickness. All data are normalized to the 4-uc sample. (c), (d) Al 2*p* and Sr 3*d* core-level spectra used for the determination of the valence band offset. Apart from slight statistical variations ($\lesssim$0.05 eV), no systematic behavior of the core-level energies with increasing LAO film thickness is observed.

from the valence band analysis. The conduction band (CB) offset is calculated to approximately 2.6 ± 0.1 eV using the optical band gaps of $\Delta_{LAO} = 5.6$ eV for LAO (Ref. 32) and $\Delta_{STO} = 3.3$ eV for STO.[33,34]

The negative sign of ΔE_{VB} means that the VBM of STO is *below* the VBM of LAO (type-II interface). While agreeing in sign, the value obtained here is significantly higher than the offset reported by other photoemission studies of PLD-grown heterostructures.[10,21,35] Note that a possible small downward bending of the STO-VBM towards the interface would imply an even larger offset directly at the interface. In contrast, from photoemission on samples grown by molecular beam epitaxy (MBE), Segal *et al*. have recently concluded on an offset value similar to ours, but of *opposite* sign, i.e., a type-I interface.[19]

IV. DISCUSSION

One of the key results of our study is certainly the apparent absence of any potential gradient in the LAO film, which is in strong contrast to the predictions of DFT calculations for perfectly stoichiometric heterostructures. Consequently, one has to think about possible extrinsic effects not covered by conventional band theory. Here, we will discuss the possible role of photoinduced carriers and oxygen vacancies.

It is well known that even ambient light creates long-lived photocarriers in LAO/STO heterostructures strongly affecting, e.g., the electrical conductivity.[36] Similar excitations may occur during the actual HAXPES measurements: As a side effect of photoelectron emission, also high-energy electron-hole pair excitations are created, with electrons and holes rapidly thermalizing down to the conduction and valence band edges, respectively. Due to the polar field in the LAO film (if existing), holes and electrons will be spatially separated and accumulated at the LAO surface and at the interface, respectively, with little chance for recombination. This out-of-equilibrium state builds up a field of opposite sign and may in saturation fully compensate the intrinsic potential gradient

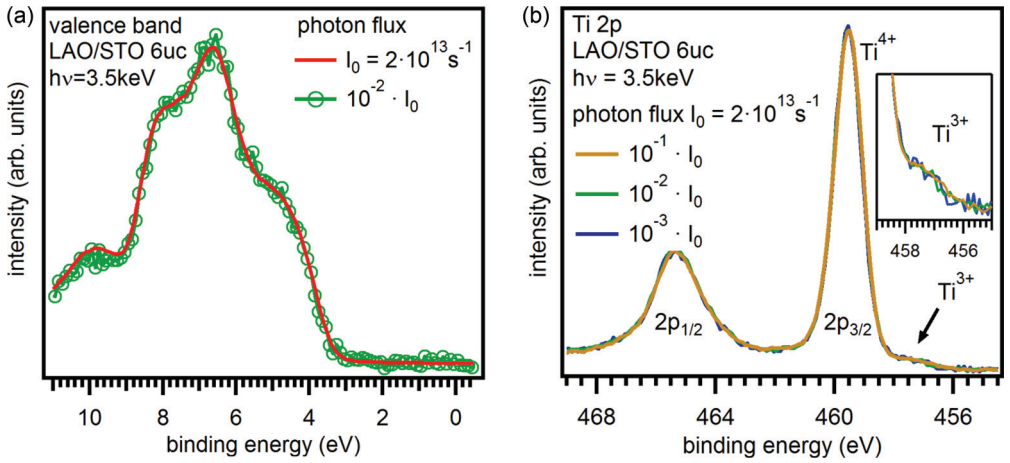

FIG. 5. (Color online) Valence band (a) and Ti $2p$ core-level (b) spectra measured with different photon beam intensities. Neither a change in valence band shape and maximum nor in the Ti^{3+} spectral weight is observable. The spectra are normalized to the same integrated peak area. The photon spot size was $\approx 2000 \times 100\ \mu m^2$.

in the LAO film.[37] It could even affect the measured values of the band alignment at the interface due to a photoinduced change of the local potential near the interface.

This mechanism is based on a distinct imbalance between formation and recombination rate of the photogenerated electrons and holes. One would thus expect it to depend strongly on x-ray intensity. In order to test this scenario, we have therefore taken a series of both valence band and Ti $2p$ core-level spectra with varying photon flux, shown in Fig. 5. Clearly, no changes are observed in shape or energy position of the valence band, when reducing the maximum photon intensity I_0 of the beamline[38] by two orders of magnitude. The same holds for the Ti $2p$ spectrum and the relative proportion of Ti^{3+} to Ti^{4+} weight, even when reducing the intensity by one order of magnitude more. Note that the chronological order of these measurements was from low to high flux, attempting to prevent early saturation. These results show that photon intensity reduction by three orders of magnitude does not lead to a detectable restoration of the internal LAO band bending nor to a notable decrease of charge carriers at the interface. In agreement with the conclusions of another recent HAXPES study,[22] our findings therefore seem to indicate that the effect of photogenerated carriers on band bending is small. However, already the weakest intensities used may be too close to saturation. Unfortunately, a further reduction of the photon flux is not feasible due to the already very low photoemission signal. Thus, we can not exclude the possibility of photocarrier-induced band flattening. We wish to remark, though, that photoemission experiments on a related heterostructure with polar discontinuity ($LaCrO_3/SrTiO_3$) *did* observe a built-in potential gradient,[16] indicating that it is principally detectable and that its absence in photoemission spectra of LAO/STO could therefore be real.

An alternative explanation for the apparent flat band situation has been provided by recent theoretical studies which allow for the presence of oxygen vacancies in the LAO film[22,26,39–41] (not to be confused with the role of vacancies in the STO substrate). In these calculations, it is found that the cost of energy associated with the generation of these defects, i.e., their enthalpy of formation, assumes a minimum at the LAO surface and that each (positively charged) oxygen vacancy leaves two electrons which are transferred to the interface. The resulting charge distribution counteracts the polar field and thus reduces its electrostatic energy. Thus, above a critical thickness it will energetically be favorable to induce oxygen defects at the LAO surface, with a positively charged (but insulating) surface and a negatively charged interface 2DES.[26,39,40] To some extent, this pictures restores the original electronic reconstruction scenario by replacing the hole states of the (experimentally not observed) metallic LAO surface band by vacancy-induced empty defect states at the surface (see also the discussion in Ref. 37). Here, we note that the generation of oxygen defects by the tip of an atomic force microscope (AFM) has also been discussed as the driving mechanism for AFM-induced switching of the 2DES.[42]

In addition, we wish to point out that our results have been obtained on samples which have been exposed to ambient atmosphere prior to the HAXPES measurements with no further surface preparation. Recent experiments show a strong influence of polar adsorbates on the conductivity of the 2DES.[43] It is therefore conceivable that, e.g., water adsorption on the LAO surface could affect the electronic structure in such a way as to behave different from the clean stoichiometric situation assumed in most DFT studies. In fact, Bristowe *et al.* have pointed out that surface protonation (e.g., by x-ray-induced or catalytic decomposition of H_2O molecules) may have an effect analogous to that of oxygen vacancies.

In Fig. 6, we summarize our results on the band arrangement in LAO/STO heterostructures, including the respective band gaps and the average values for VBM position and VB offset. The most important results are the VB offset being independent of LAO film thickness and the apparent absence of a strong internal field in LAO, concluded from both the analysis of the VB spectra as well as from the measured core-level energy differences in LAO and STO (cf. Table I). Other photoemission studies have also analyzed the relative core-level energies, e.g., $\Delta E(\mathrm{Sr}\ 3d_{5/2} - \mathrm{La}\ 4d_{5/2})$ (Refs. 19 and 22) or $\Delta E(\mathrm{Al}\ 2p - \mathrm{Sr}\ 3d_{5/2})$ (Ref. 20) and observed, in agreement with our findings, much smaller variations with LAO film thickness than one would expect for the predicted strong potential gradient.

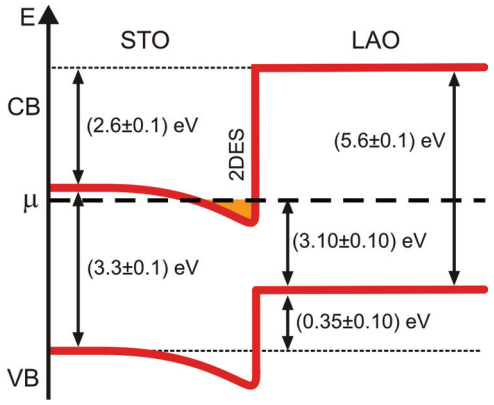

FIG. 6. (Color online) Band alignment in the LAO/STO heterostructure as determined by photoemission. A remarkable result from our HAXPES study is the flat band behavior in the LAO film and the VB offset, which are both independent of the number of LAO layers.

On the other hand, and in contrast to our data, the remaining ΔE behavior has been reported to systematically depend on the number of LAO layers and attributed to a small residual band bending within the LAO film. However, such an interpretation is ambiguous, as one can not clearly distinguish between a thickness-related change of the band alignment and an energy shift due to the increasing built-in field. Furthermore, while the values of ΔE for samples above and below the critical thickness differ significantly suggesting the systematic trend, the variations of ΔE for samples above the critical thickness are small within the error bars. However, samples with only 1 or 2 uc of LAO should be highly insulating, thus photoemission on them being strongly affected by charging. This is indeed the reason why, e.g., for our 2-uc sample a precise VB offset analysis was not feasible and reliable core-level energies could not be determined.

The apparent noncharging of subcritical LAO films in other photoemission studies suggests a higher density of oxygen vacancies in the STO substrates and hence larger residual conductivity. In contrast, for our sample set we have taken special care to minimize the oxygen vacancy density near the interface by the extra post-oxidation step.[44] This oxygen vacancy conditioning is independent of LAO film thickness and could be a reasonable explanation for the nearly constant VB offset in our samples.

Note that a recent report of a significant potential gradient observed in tunneling and capacitance experiments on LAO/STO (Ref. 45) is not directly comparable to our present results. In those experiments, a metal electrode was attached to the LAO surface of the heterojunctions. It is well known from both experiment and theory that the electronic structure of capped LAO/STO can be quite different[46–48] from heterostructures with free surfaces, as studied here.

V. SUMMARY

We have presented a detailed study of the band arrangement in LAO/STO heterostructures by using hard x-ray photoelectron spectroscopy. Our data taken on *ex situ* grown samples show apparent flat band behavior in the LAO film, in agreement with previous photoemission experiments, but at variance with the DFT calculations for stoichiometric heterostructures. Modified electronic reconstruction scenarios involving oxygen vacancies at the LAO surface or the influence of polar surface adsorbates could provide a possible explanation for the absence of the potential gradient. Alternatively, the experimental observations could also result from a photon-induced nonequilibrium charge imbalance. Furthermore, we have determined the band offset between the VBM of LAO and STO and found it to be independent of the LAO film thickness. However, the absolute values partially disagree with previous photoemission experiments, possibly related to subtle differences in heterostructure preparation conditions. Clearly, more systematic studies on the effect of epitaxial growth parameters (in particular concerning the oxygen stoichiometry) and the difference between *in situ* and *ex situ* prepared samples are needed.

ACKNOWLEDGMENTS

We thank H. Boschker, T. Kopp, and N. Pavlenko for fruitful discussions and gratefully acknowledge financial support by the Deutsche Forschungsgemeinschaft (FOR 1162 and TRR 80), and Deutsches Elektronen-Synchrotron (DESY). The HAXPES instrument at beamline P09 is jointly operated by the University of Würzburg (R. Claessen), the University of Mainz (C. Felser), and DESY. Funding by the Federal Ministry of Education and Research (BMBF) under Contracts No. 05KS7UM1, No. 05K10UMA, No. 05KS7WW3, and No. 05K10WW1 is gratefully acknowledged.

*claessen@physik.uni-wuerzburg.de

[1] A. Ohtomo and H. Y. Hwang, Nature (London) **427**, 423 (2004).
[2] S. Thiel, G. Hammerl, A. Schmehl, C. W. Schneider, and J. Mannhart, Science **313**, 1942 (2006).
[3] N. Reyren, S. Thiel, A. D. Caviglia, L. F. Kourkoutis, G. Hammerl, C. Richter, C. W. Schneider, T. Kopp, A.-S. Ruetschi, D. Jaccard, M. Gabay, D. A. Müller, J.-M. Triscone, and J. Mannhart, Science **317**, 1196 (2007).
[4] A. D. Caviglia, S. Gariglio, N. Reyren, D. Jaccard, T. Schneider, M. Gabay, S. Thiel, G. Hammerl, J. Mannhart, and J.-M. Triscone, Nature (London) **456**, 624 (2008).
[5] L. Li, C. Richter, J. Mannhart, and R. Ashoori, Nat. Phys. **7**, 762 (2011).
[6] J. A. Bert, B. Kalisky, C. Bell, M. Kim, Y. Hikita, H. Y. Hwang, and K. A. Moler, Nat. Phys. **7**, 767 (2011).
[7] B. Kalisky, J. A. Bert, B. B. Klopfer, C. Bell, H. K. Sato, M. Hosoda, Y. Hikita, H. Y. Hwang, and K. A. Moler, Nat. Commun. **3**, 922 (2012).
[8] A. Brinkman, M. Huijben, M. van Zalk, J. Huijben, U. Zeitler, J. C. Maan, W. G. van der Wiel, G. Rijnders, D. H. A. Blank, and H. Hilgenkamp, Nat. Mater. **6**, 493 (2007).
[9] P. R. Willmott, S. A. Pauli, R. Herger, C. M. Schlepütz, D. Martoccia, B. D. Patterson, B. Delley, R. Clarke, D. Kumah, C. Cionca, and Y. Yacoby, Phys. Rev. Lett. **99**, 155502 (2007).
[10] S. Chambers, M. Engelhard, V. Shutthanandan, Z. Zhu, T. Droubay, L. Qiao, P. Sushko, T. Feng, H. Lee, T. Gustafsson, E. Garfunkel,

A. Shah, J.-M. Zuo, and Q. Ramasse, Surf. Sci. Rep. **65**, 317 (2010).
[11]N. Nakagawa, H. Y. Hwang, and D. A. Müller, Nat. Mater. **5**, 204 (2006).
[12]M. Basletic, J.-L. Maurice, C. Carrétéro, G. Herranz, O. Copie, M. Bibes, E. Jacquet, K. Bouzehouane, S. Fusil, and A. Barthélémy, Nat. Mater. **7**, 621 (2008).
[13]M. Sing, G. Berner, K. Goss, A. Müller, A. Ruff, A. Wetscherek, S. Thiel, J. Mannhart, S. A. Pauli, C. W. Schneider, P. R. Willmott, M. Gorgoi, F. Schäfers, and R. Claessen, Phys. Rev. Lett. **102**, 176805 (2009).
[14]R. Pentcheva and W. E. Pickett, Phys. Rev. Lett. **102**, 107602 (2009).
[15]Y. Li and J. Yu, J. Appl. Phys. **108**, 013701 (2010).
[16]S. A. Chambers, L. Qiao, T. C. Droubay, T. C. Kaspar, B. W. Arey, and P. V. Sushko, Phys. Rev. Lett. **107**, 206802 (2011).
[17]C. W. Schneider, S. Thiel, G. Hammerl, C. Richter, and J. Mannhart, Appl. Phys. Lett. **89**, 122101 (2006).
[18]C. J. Powell and A. Jablonski, *NIST Electron Inelastic-Mean-Free-Path Database* - Version 1.2 (National Institute of Standards and Technology, Gaithersburg, MD, 2010).
[19]Y. Segal, J. H. Ngai, J. W. Reiner, F. J. Walker, and C. H. Ahn, Phys. Rev. B **80**, 241107 (2009).
[20]M. Takizawa, S. Tsuda, T. Susaki, H. Y. Hwang, and A. Fujimori, Phys. Rev. B **84**, 245124 (2011).
[21]G. Drera, G. Salvinelli, A. Brinkman, M. Huijben, G. Koster, H. Hilgenkamp, G. Rijnders, D. Visentin, and L. Sangaletti, Phys. Rev. B **87**, 075435 (2013).
[22]E. Slooten, Z. Zhong, H. J. A. Molegraaf, P. D. Eerkes, S. de Jong, F. Massee, E. van Heumen, M. K. Kruize, S. Wenderich, J. E. Kleibeuker, M. Gorgoi, H. Hilgenkamp, A. Brinkman, M. Huijben, G. Rijnders, D. H. A. Blank, G. Koster, P. J. Kelly, and M. S. Golden, Phys. Rev. B **87**, 085128 (2013).
[23]J. Lee and A. A. Demkov, Phys. Rev. B **78**, 193104 (2008).
[24]R. Pentcheva and W. E. Pickett, Phys. Rev. B **78**, 205106 (2008).
[25]K. Janicka, J. P. Velev, and E. Y. Tsymbal, Phys. Rev. Lett. **102**, 106803 (2009).
[26]Y. Li, S. N. Phattalung, S. Limpijumnong, J. Kim, and J. Yu, Phys. Rev. B **84**, 245307 (2011).
[27]M. Salluzzo, J. C. Cezar, N. B. Brookes, V. Bisogni, G. M. De Luca, C. Richter, S. Thiel, J. Mannhart, M. Huijben, A. Brinkman, G. Rijnders, and G. Ghiringhelli, Phys. Rev. Lett. **102**, 166804 (2009).
[28]A. Sorokine, D. Bocharov, S. Piskunov, and V. Kashcheyevs, Phys. Rev. B **86**, 155410 (2012).
[29]Z. S. Popović, S. Satpathy, and R. M. Martin, Phys. Rev. Lett. **101**, 256801 (2008).
[30]E. A. Kraut, R. W. Grant, J. R. Waldrop, and S. P. Kowalczyk, Phys. Rev. Lett. **44**, 1620 (1980).
[31]E. A. Kraut, R. W. Grant, J. R. Waldrop, and S. P. Kowalczyk, Phys. Rev. B **28**, 1965 (1983).
[32]S.-G. Lim, S. Kriventsov, T. N. Jackson, J. H. Haeni, D. G. Schlom, A. M. Balbashov, R. Uecker, P. Reiche, J. L. Freeouf, and G. Lucovsky, J. Appl. Phys. **91**, 4500 (2002).
[33]K. van Benthem, C. Elsässer, and R. H. French, J. Appl. Phys. **90**, 6156 (2001).
[34]M. I. Cohen and R. F. Blunt, Phys. Rev. **168**, 929 (1968).
[35]L. Qiao, T. Droubay, T. Kaspar, P. Sushko, and S. Chambers, Surf. Sci. **605**, 1381 (2011).
[36]M. Huijben, G. Rijnders, D. H. A. Blank, S. Bals, S. V. Aert, J. Verbeeck, G. V. Tendeloo, A. Brinkman, and H. Hilgenkamp, Nat. Mater. **5**, 556 (2006).
[37]G. Berner, M. Sing, H. Fujiwara, A. Yasui, Y. Saitoh, A. Yamasaki, Y. Nishitani, A. Sekiyama, N. Pavlenko, T. Kopp, C. Richter, J. Mannhart, S. Suga, and R. Claessen, Phys. Rev. Lett. **110**, 247601 (2013).
[38]J. Strempfer, S. Francoual, D. Reuther, D. K. Shukla, A. Skaugen, H. Schulte-Schrepping, T. Kracht, and H. Franz, J. Synchrotron Radiat. **20**, 541 (2013).
[39]N. C. Bristowe, P. B. Littlewood, and E. Artacho, Phys. Rev. B **83**, 205405 (2011).
[40]Z. Zhong, P. X. Xu, and P. J. Kelly, Phys. Rev. B **82**, 165127 (2010).
[41]N. Pavlenko, T. Kopp, E. Y. Tsymbal, J. Mannhart, and G. A. Sawatzky, Phys. Rev. B **86**, 064431 (2012).
[42]C. Cen, S. Thiel, G. Hammerl, C. W. Schneider, K. E. Andersen, C. S. Hellberg, J. Mannhart, and J. Levy, Nat. Mater. **7**, 298 (2008).
[43]Y. Xie, Y. Hikita, C. Bell, and H. Y. Hwang, Nat. Commun. **2**, 494 (2011).
[44]A. Müller, H. Boschker, F. Pfaff, G. Berner, S. Thiess, W. Drube, G. Koster, G. Rijnders, D. H. A. Blank, M. Sing, and R. Claessen (unpublished).
[45]G. Singh-Bhalla, C. Bell, J. Ravichandran, W. Siemons, Y. Hikita, S. Salahuddin, A. F. Hebard, H. Y. Hwang, and R. Ramesh, Nat. Phys. **7**, 80 (2011).
[46]R. Pentcheva, M. Huijben, K. Otte, W. E. Pickett, J. E. Kleibeuker, J. Huijben, H. Boschker, D. Kockmann, W. Siemons, G. Koster, H. J. W. Zandvliet, G. Rijnders, D. H. A. Blank, H. Hilgenkamp, and A. Brinkman, Phys. Rev. Lett. **104**, 166804 (2010).
[47]R. Arras, V. G. Ruiz, W. E. Pickett, and R. Pentcheva, Phys. Rev. B **85**, 125404 (2012).
[48]B. Förg, C. Richter, and J. Mannhart, Appl. Phys. Lett. **100**, 053506 (2012).